

# Thermal lens study in diode pumped $N_g$ - and $N_p$ -cut Nd:KGd(WO<sub>4</sub>)<sub>2</sub> laser crystals

P.A. Loiko<sup>1</sup>, K.V. Yumashev<sup>1</sup>, N.V. Kuleshov<sup>1</sup>, V.G. Savitski<sup>2,\*</sup>, S. Calvez<sup>2</sup>, D. Burns<sup>2</sup>,  
A.A. Pavlyuk<sup>3</sup>

<sup>1</sup> Institute for Optical Materials and Technologies, Belarussian National Technical University, 65 Nezavisimosti Ave., bldg. 17, Minsk, 220013, Belarus

<sup>2</sup> Institute of Photonics, University of Strathclyde, Glasgow G4 0NW, UK

<sup>3</sup> Institute of Inorganic Chemistry, Siberian Branch of Russian Academy of Sciences, 3 Lavrentyev Ave., Novosibirsk, Russia 630090

\*vasili.savitski@strath.ac.uk

**Abstract.** A comparative study of thermal lensing effect in diode laser pumped  $N_g$ - and  $N_p$ -cut Nd:KGd(WO<sub>4</sub>)<sub>2</sub> (KGW) laser crystals was performed for laser emission polarized along the principle refractive axis,  $N_m$ . The thermal lens in the  $N_g$ -cut Nd: KGW was found to be weakly astigmatic with a positive refractive power for both the  $N_m$ - and  $N_p$ -directions. For  $N_p$ -cut Nd:KGW, strong astigmatism was observed and the refractive powers in the  $N_g$ - and  $N_m$ -directions had opposing signs. The degree of astigmatism was found to be considerably weaker for the  $N_g$ -cut Nd:KGW in comparison with the  $N_p$ -cut one: 0.35 dptr/(W/cm<sup>2</sup>) and 2.85 dptr/(W/cm<sup>2</sup>), respectively. The ratio of the thermal lens refractive powers in the planes parallel and perpendicular to the laser emission polarisation were measured as + 1.4 and -0.425 for  $N_g$ - and  $N_p$ -cut Nd:KGW respectively.

© 2009 Optical Society of America

OCIS codes: (140.3480) Lasers, diode-pumped; (140.6810) Thermal effects; (140.3530) Lasers, neodymium.

---

## References and links

1. A. A. Kaminskii, A. A. Pavlyuk, P. V. Klevtsov, I. F. Balashov, V. A. Berenberg, S. E. Sarldsov, and V. A. Fedorov, "M. V. Petrov and V. V. Lyubchenko, "Stimulated radiation of monoclinic crystals of KY(WO<sub>4</sub>)<sub>2</sub> and KGd(WO<sub>4</sub>)<sub>2</sub> with Ln<sup>3+</sup> ions," *Izv. Akad. Nauk SSSR*, Ser. Neorgan. Mater. **13**, 582 (1977).
2. A. A. Kaminskii, A. I. Bodretsova, A. G. Petrosyan, and A. A. Pavlyuk, "New quasi-cw pyrotechnically pumped crystal lasers," *Sov. J. Quantum Electron.* **13**(7), 975–976 (1983).
3. A. A. Kaminskii, H. R. Verdún, W. Koechner, F. A. Kuznetsov, and A. A. Pavlyuk, "Efficient single-mode cw lasers based on monoclinic double potassium-(rare earth) tungstenate crystals containing Nd<sup>3+</sup> ions with semiconductor-laser pumping," *Sov. J. Quantum Electron.* **22**(10), 875–877 (1992).
4. J. Findeisen, H. J. Eichler, and A. A. Kaminskii, "Efficient Picosecond Pb(WO<sub>4</sub>)<sub>2</sub> and Two-Wavelength KGd(WO<sub>4</sub>)<sub>2</sub> Raman Lasers in the IR and Visible," *IEEE J. Quantum Electron.* **35**(2), 173–178 (1999).
5. A. A. Kaminskii, J. B. Gruber, S. N. Bagaev, K. Ueda, U. Hommerich, J. T. Seo, D. Temple, B. Zandi, A. A. Kornienko, E. B. Dunina, A. A. Pavlyuk, R. F. Klevtsova, and F. A. Kuznetsov, "Optical spectroscopy and visible stimulated emission of Dy<sup>3+</sup> ions in monoclinic  $\alpha$ -KY(WO<sub>4</sub>)<sub>2</sub> and  $\alpha$ -KGd(WO<sub>4</sub>)<sub>2</sub> crystals," *Phys. Rev. B* **65**(12), 125108 (2002).
6. O. Musset, and J. P. Boquillon, "Comparative laser study of Nd:KGW and Nd:YAG near 1.3  $\mu$ m," *Appl. Phys. B* **64**(4), 503–506 (1997).
7. N. S. Ustimenko, and A. V. Gulin, "New self-frequency converted Nd<sup>3+</sup>:KGd(WO<sub>4</sub>)<sub>2</sub> Raman lasers," *Quantum Electron.* **32**(3), 229–231 (2002) (REMOVED HYPERLINK FIELD).
8. H. Jianhong, L. Jipeng, S. Rongbing, L. Jinghui, Z. Hui, X. Canhua, S. Fei, L. Zongzhi, Z. Jian, Z. Wenrong, and L. Wenxiong, "Short pulse eye-safe laser with a stimulated Raman scattering self-conversion based on a Nd:KGW crystal," *Opt. Lett.* **32**(9), 1096–1098 (2007).
9. T. T. Basiev, "New crystals for Raman lasers," *Phys. Solid State* **47**(8), 1400–1405 (2005).
10. D. Sakaizawa, C. Nagasawa, T. Nagai, M. Abo, Y. Shibata, and M. Nakazato, "Stimulated Raman Scattering Laser Oscillation around 1.6 $\mu$ m Carbon Dioxide Absorption Line," *Jpn. J. Appl. Phys.* **47**(3), 1612–1614 (2008).
11. A. A. Demidovich, A. P. Shkadarevich, M. B. Danailov, P. Apai, T. Gasmii, V. P. Gribkovskii, A. N. Kuzmin, G. I. Ryabtsev, and L. E. Batay, "Comparison of cw laser performance of Nd:KGW, Nd:YAG, Nd:BEL, and Nd:YVO<sub>4</sub> under laser diode pumping," *Appl. Phys. B* **67**(1), 11–15 (1998).

12. W. Lubeigt, M. Griffith, L. Laycock, and D. Burns, "Reduction of the time-to-full-brightness in solid-state lasers using intra-cavity adaptive optics," *Opt. Express* **17**(14), 12057–12069 (2009).
13. I. V. Mochalov, "Laser and nonlinear properties of the potassium gadolinium tungstate laser crystal  $\text{KGd}(\text{WO}_4)_2\text{:Nd}^{3+}$  (KGW:Nd)," *Opt. Eng.* **36**(6), 1660–1669 (1997).
14. V. V. Filippov, N. V. Kuleshov, and I. T. Bodnar, "Negative thermo-optical coefficients and athermal directions in monoclinic  $\text{KGd}(\text{WO}_4)_2$  and  $\text{KY}(\text{WO}_4)_2$  laser host crystals in the visible region," *Appl. Phys. B* **87**(4), 611–614 (2007).
15. S. Biswal, S. P. O'Connor, and S. R. Bowman, "Thermo-optical parameters measured in ytterbium-doped potassium gadolinium tungstate," *Appl. Opt.* **44**(15), 3093–3097 (2005).
16. K. V. Yumashev, V. G. Savitski, N. V. Kuleshov, A. A. Pavlyuk, D. D. Molotkov, and A. L. Protaseny, "Laser performance of  $N_g$ -cut flash-lamp pumped Nd:KGW at high repetition rates," *Appl. Phys. B* **89**(1), 39–43 (2007).
17. F. Hoos, S. Li, T. P. Meyrath, B. Braun, and H. Giessen, "Thermal lensing in an end-pumped Yb:KGW slab laser with high power single emitter diodes," *Opt. Express* **16**(9), 6041–6049 (2008).
18. W. Koehner, *Solid-state laser engineering* (Springer, New York 2006).
19. S. Agarwal, D. J. Apple, L. Burrato, J. L. Alio, S. K. Pandey, and A. Agarwal, *Textbook of Ophthalmology*, vol.1 (Jaypee Brothers Medical Publishers (P) Ltd, New Delhi, 2002).
20. A. A. Pavlyuk, Y. V. Vasiliev, L. Y. Kharchenko, and F. A. Kuznetsov, Proceedings of the APSAM-92, Asia Pacific Society for Advanced Materials, Shanghai, 26–29 April 1992 (1993), pp. 164–171.
21. M. C. Pujol, M. Sol'e, J. Massons, J. Gavalda, X. Solans, C. Zaldo, F. Díaz, and M. Aguiló, J. Gavalda, X. Solans, C. Zaldo, F. Díaz, M. Aguiló, "Structural study of monoclinic  $\text{KGd}(\text{WO}_4)_2$  and effects of lanthanide substitution," *J. Appl. Cryst.* **34**(1), 1–6 (2001).
22. N. Hodgson, and H. Weber, *Optical resonators: fundamentals, advanced concepts and applications* (Springer, London 1997).
23. J. E. Hellström, S. Bjurshagen, V. Pasiskevicius, J. Liu, V. Petrov, and U. Griebner, "Efficient Yb:KGW lasers end-pumped by high-power diode bars," *Appl. Phys. B* **83**(2), 235–239 (2006).
24. M. Shimosegawa, T. Omatsu, A. Hasegawa, M. Tateta, and I. Ogura, "Transient thermal lensing measurement in a laser diode pumped  $\text{Nd}_x\text{Y}_{1-x}\text{Al}_3(\text{BO}_3)_4$  laser using a holographic shearing interferometer," *Opt. Commun.* **140**(4–6), 237–241 (1997).
25. M. C. Pujol, M. Rico, C. Zaldo, M. Sol'e, V. Nikolov, X. Solans, F. M. Aguiló, and F. Díaz, "Díaz, "Crystalline structure and optical spectroscopy of  $\text{Er}^{3+}$ -doped  $\text{KGd}(\text{WO}_4)_2$  single crystals," *Appl. Phys. B* **68**(2), 187–197 (1999).

## 1. Introduction

Neodymium-doped  $\text{KGd}(\text{WO}_4)_2$  (KGW) is a well known laser material with extensively investigated spectroscopic properties (see [1–5] and references therein). Nd:KGW has good prospects for self-Raman conversion to 1.54  $\mu\text{m}$  [7,8] due to the relatively high emission cross-section at  $\sim 1.35 \mu\text{m}$  ( $7.6 \times 10^{-20} \text{ cm}^2$  [6]) also in combination with a high Raman gain coefficient (up to 4.4 cm/GW [1]). This is of specific relevance when the laser is operated in the picosecond time domain [9]. This so-called 'eye-safe' spectral range is attractive for realization of high frequency range finders at 1.54  $\mu\text{m}$ , and atmospheric  $\text{CO}_2$  monitoring [10] at 1.57–1.6  $\mu\text{m}$  (via Raman conversion in  $\text{Ba}(\text{NO}_3)_2$ ). Power scaling in tungstates is, however, limited compared to Nd:YAG lasers, as the thermal conductivity coefficients are approximately 3 times lower [5]. Commercially available  $N_p$ -cut Nd:KGW possess strong cylindrical thermal lensing [11], which is difficult to compensate by cavity design alone or by means of adaptive optics [12]. The output power obtainable from tungstate lasers under high power pumping is therefore substantially reduced. Moreover, the poor thermo-optical characteristics typical of tungstates limit its application as effective Raman crystal specifically for high-energy nanosecond pulse operation.

However, there exists a distinctive feature of the KGW crystal which may significantly improve this performance, namely, the negative coefficients of the temperature dependence of the refractive index,  $dn/dT$ , for some light polarizations and propagation directions (e.g.  $-0.8 \times 10^{-6} \text{ K}^{-1}$  for  $k//N_p$ ,  $E//N_m$ ) [13–15]. In fact, exploitation of this feature has led to higher output powers being obtained at  $\sim 1 \mu\text{m}$  compared with similar Nd:YAG lasers under high power flash-lamp pumping - average output powers of 40 W at 1.4 kW of pumping was obtained from an  $N_g$ -cut Nd:KGW crystal laser which compares favourably with 15 W of output from a similarly configured Nd:YAG laser [16]. In the same configuration, the more conventional  $N_p$ -cut Nd:KGW crystal laser ceased operating at only 0.5 kW of average pump power. In another demonstration, an end-pumped  $N_g$ -cut Yb:KGW crystal produced  $\sim 5$  W of laser output power with a near-diffraction limited beam quality [17] under 18 W pumping. The key point of these examples was the exploitation of the special, often called *athermal*,

direction of propagation within the KGW crystal, where the temperature- and stress-dependent refractive indices compensate each other, resulting in significantly lower thermal lensing [13–15]. The direction along the principle refractive axis  $N_g$  has been identified as being one of these *athermal* directions, although other orientations are also possible [13,15]. Such ‘smart-cut’ tungstate crystals therefore show great promise for flexible thermal management, giving access to a wider range of applications including self-Raman conversion.

In this paper, we will compare the thermal lensing effect in two diode laser pumped Nd:KGW lasers having the light propagation direction along the principle refractive axes  $N_g$  and  $N_p$  (hereafter denoted as  $N_g$ -cut and  $N_p$ -cut Nd:KGW crystals, respectively). As a result the thermal lensing sensitivity factors,  $M$ , for these crystals can then be determined and the degree of thermal lens’ astigmatism for both crystals can be calculated and compared. This factor  $M$  - the rate at which the thermal lens refractive power varies with pump power intensity - then provides a convenient measure to compare the induced thermal lensing in different laser crystals and orientations [18]. The degree of astigmatism here is the difference between the values of thermal lens refractive power per pump intensity (i.e. between the values of the factor  $M$ ) in the plane of polarization ( $N_m$ ) and in the perpendicular plane - a typical measure of astigmatism in, for example, ophthalmology [19].

## 2 Experimental

The Nd:KGW crystal was grown from the flux by using  $K_2W_2O_7$  as a solvent. The modified Czochralski technique was used under conditions of low thermal gradient [20]. The  $N_p$ -cut Nd:KGW laser gain medium was grown along the crystallographic axis  $b$  which is parallel to the principle refractive axis  $N_p$ , whereas, the  $N_g$ -cut Nd:KGW material was grown along the crystallographic axis  $c$  (the angle between the  $c$ - and  $N_g$ -axis is  $21.5^\circ$  [21]). Other properties of the  $N_p$ - and  $N_g$ -cut Nd:KGW crystals were identical.

In all the experiments described here, the  $N_g$ -cut and  $N_p$ -cut Nd:KGW crystals had a doping level of 7 at. % neodymium and a length of  $l = 1.9$  mm. One polished end-face served as a flat laser cavity mirror - a multi-layer dielectric coating was applied to this face to provide both a high-reflectivity at the laser wavelength of  $1.35 \mu\text{m}$  and antireflection at  $808$  nm (i.e the pump wavelength). The coating also provided minimal reflectivity at  $1.067 \mu\text{m}$  to prevent any parasitic laser oscillation at this wavelength. The other crystal end-face was antireflection-coated for both  $1.35$  and  $1.06 \mu\text{m}$ . The laser crystal was mounted on a thermo-electric cooled brass plate and the temperature was controlled to  $15^\circ\text{C}$ . Finally, the linear laser cavity was terminated by a concave output coupler having a radius of curvature of  $R = 50$  mm and a reflectivity of 99% at  $1.35 \mu\text{m}$ .

The experiments reported here were intentionally performed at a laser oscillation wavelength of  $1.35 \mu\text{m}$  due to the thermal effects in the Nd:KGW laser crystal being higher at this wavelength in comparison to oscillation at  $1.067 \mu\text{m}$ . The diode lasers emitting at a wavelength of  $808$  nm were used as the end-pumping sources for the laser set-up. The  $N_p$ -cut Nd:KGW crystal was quasi-continuously pumped with the emission being linearly polarized along the  $N_m$  optical indicatrix axis. Pump radiation was focused into the crystal to a spot with the diameter of  $75 \mu\text{m}$ . The  $N_g$ -cut Nd:KGW crystal was continuously pumped by the fiber-coupled laser diode with unpolarized emission. The pump spot into the  $N_g$ -cut Nd:KGW crystal was symmetric with the diameter of  $150 \mu\text{m}$ .

Length of the crystals ( $1.9$  mm) and doping concentration (7 at. %) provided 98.8% absorption of unpolarised pump emission at  $808$  nm and  $\sim 99.2\%$  absorption of the polarized pump emission at the same wavelength. We believe the difference in absorption coefficients for polarizations along different crystal axes makes negligible impact on the measurements. The emission of the  $N_g$ - and  $N_p$ -cut Nd:KGW lasers is polarised along the  $N_m$ -axis, and the lasers were configured to emit a fundamental TEM<sub>00</sub> spatial mode.

Resonator lengths of  $26$  mm for the  $N_g$ -cut Nd:KGW and of  $49$  mm for the  $N_p$ -cut Nd:KGW crystals were chosen to provide the highest output power. The reason for different values of the resonator length will be given below.

Different techniques can be applied to determine thermal lens in laser crystals: measurements of the changes of the output beam characteristics for stable resonator operating at TEM<sub>00</sub> mode [11,17] and for the resonator close to instability region [16,22]; measurements of the changes in the spatial profile of the probe beam which is passed through a gain medium [22,23]; interferometric measurements [13,24].

Two methods were employed in the present paper to determine the sensitivity factor  $M$ . In the first method, the output beam characteristics are measured with respect to the distance from the output coupler at different pump intensities,  $P_p/\pi w_p^2$ , where  $P_p$  and  $w_p$  are the pump power and the  $(1/e^2)$  Gaussian radius of the pump beam, respectively. The measurements are performed by the knife edge method [22] in two directions: parallel to the  $N_m$ - and  $N_g$ -axes for the  $N_p$ -cut Nd:KGW laser crystal, and parallel to the  $N_m$ - and  $N_p$ -axes for the  $N_g$ -cut Nd:KGW system. Measured output beam size dependencies on the distance from the output coupler are then simulated using the ABCD matrix method [18]. In these calculations, thermo-optical distortions within the gain medium are described by an astigmatic thermal lens of refractive power,  $D$ , which is dependent on the pump intensity. The sensitivity factor  $M$  is then obtained from the slope of the dependence of thermal lens refractive power versus the pump intensity.

The second method is based on the observation of substantial changes in the spatial and power characteristics of the laser output indicative of the laser resonator becoming unstable due to an action of thermal lensing [22]. Here, the output power of the laser is monitored as a function of the pump intensity at a given cavity length. The pump intensity,  $(P_p/\pi w_p^2)_c$ , at which the output power begins to reduce is assumed to induce in the gain medium a thermal lens with a critical refractive power,  $D_c$ , corresponding to the edge of the cavity stability on the  $g_1^*g_2^*$  diagram [18,22]. The sensitivity factor  $M$  is then calculated as the ratio of this critical refractive power  $D_c$  to the value of  $(P_p/\pi w_p^2)_c$ . It should be noted that, in the case of an astigmatic thermal lens, this method provides information on the sensitivity factor in one propagation plane only – i.e. the plane that approaches the stability edge at the least pump power.

### 3 Results and discussion

The typical measured dependence of the output beam mode diameter with distance from the output coupler for both the  $N_g$ - and  $N_p$ -cut Nd:KGW lasers are shown in Fig. 1. From these data, it is clear that for the  $N_g$ -cut Nd:KGW laser, the output beam suffered compression in both  $N_m$ - and  $N_p$ -directions with increasing pump intensity (Fig. 1(a, b)). The compression along the  $N_m$ -direction was notably greater than that observed along the  $N_p$ -axis. However, in the case of the  $N_p$ -cut Nd:KGW laser (Fig. 1(c, d)) as the pump intensity increases, the size of the output beam decreases along the  $N_m$  direction but increases along  $N_p$ . It follows from a calculation of the laser mode behaviour outside the laser cavity that a decrease in the mode size corresponds to an inducted positive thermal lens within the gain crystal, whereas a defocusing lens induces an increase in the mode size. From this ABCD matrix analysis the data of Fig. 1 can be fitted to values of the induced refractive power of the gain crystal, and these are shown as solid, dashed and dotted lines in the figure. Therefore, it is clear that the thermal lenses induced in the  $N_g$ - and  $N_p$ -cut Nd:KGW active elements are both astigmatic. For the  $N_g$ -cut Nd:KGW, the refractive powers of the thermal lens are distinguished in magnitude in the  $N_m$ - and  $N_p$ -directions, however, they both have the same sign (i.e. positive). This is in contrast to the  $N_p$ -cut Nd:KGW case where the refractive powers have opposite signs in the  $N_m$ - and  $N_g$ -directions (positive and negative respectively).

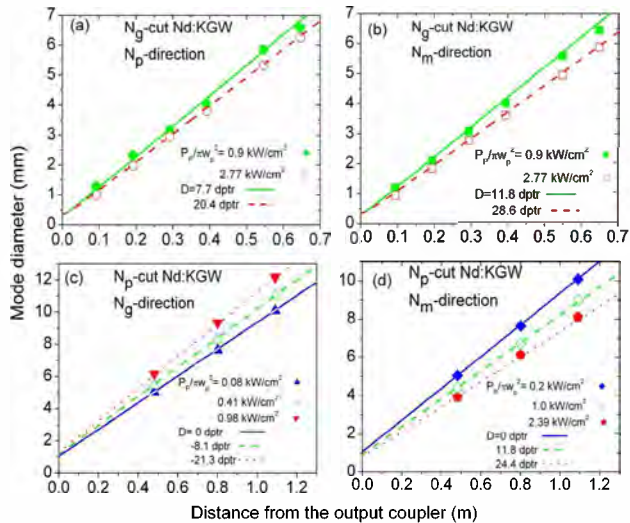


Fig. 1. Dependence of the output beam mode diameter as a function of the distance from the output coupler at different pump intensities ( $P_p/\pi w_p^2$ ) for the  $N_g$ - and  $N_p$ -cut Nd:KGW lasers (cavity length is 26 mm for the  $N_g$ -cut Nd:KGW laser and 49 mm for the  $N_p$ -cut Nd:KGW one). Symbols – experimental data. Lines – results of calculations according to the ABCD-method.

The dependences of the thermal lensing as a function of pump intensity for the  $N_g$ - and  $N_p$ -cut Nd:KGW crystals were measured and are shown in Fig. 2. As expected from theory [22], these dependences are linear with pump intensity, and from the respective gradients of the data the thermal lensing sensitivity factors  $M$  can be calculated - these were found to be, in units of dioptric power per ( $\text{W}/\text{cm}^2$ ):

$$(M_{N_g\text{-cut}})_{N_m} = 1.2 \times 10^{-2} \text{ (} N_g\text{-cut Nd:KGW, } N_m\text{-direction),}$$

$$(M_{N_g\text{-cut}})_{N_p} = 0.85 \times 10^{-2} \text{ (} N_g\text{-cut Nd:KGW, } N_p\text{-direction),}$$

$$(M_{N_p\text{-cut}})_{N_m} = 0.85 \times 10^{-2} \text{ (} N_p\text{-cut Nd:KGW, } N_m\text{-direction), and}$$

$$(M_{N_p\text{-cut}})_{N_g} = -2.0 \times 10^{-2} \text{ (} N_p\text{-cut Nd:KGW, } N_g\text{-direction).}$$

The degree of astigmatism [19] for the  $N_p$  and  $N_g$ -cut Nd:KGW crystals can now be calculated as a difference in corresponding  $M$  factors in the plane of polarization ( $N_m$ ) and in the perpendicular plane:

$$N_g\text{-cut Nd:KGW: } 0.35 \text{ dptr}/(\text{W}/\text{cm}^2);$$

$$N_p\text{-cut Nd:KGW: } 2.85 \text{ dptr}/(\text{W}/\text{cm}^2).$$

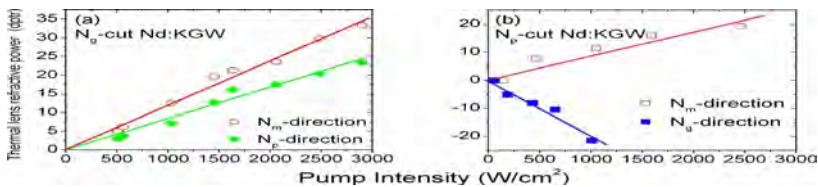


Fig. 2. The dependence of thermal lensing on pump intensity ( $P_p/\pi w_p^2$ ) in diode laser pumped (a)  $N_g$ -cut - and (b)  $N_p$ -cut Nd:KGW lasers. Symbols – experimental data on thermal lens refractive power. Solid lines – linear fit to the data.

Resonator with the length of 49 mm for the  $N_p$ -cut Nd:KGW provided the widest stability region against the negative thermal lensing (which was found to be stronger in this crystal than the positive one), while the  $N_g$ -cut Nd:KGW laser with the cavity length of 26 mm was

about two times more stable against positive thermal lensing in comparison with the cavity length of 49 mm (see the calculated critical values of the thermal lens refractive power below). The difference in the resonator length for two Nd:KGW crystals does not influence the measurements of the thermal lens, as the calculations of the beam profile outside the cavity are performed separately for the given cavity length.

The measured output power dependence on pump intensity ( $P_p/\pi w_p^2$ ) for the  $N_p$ -cut and  $N_g$ -cut Nd:KGW lasers is presented in Fig. 3(a).

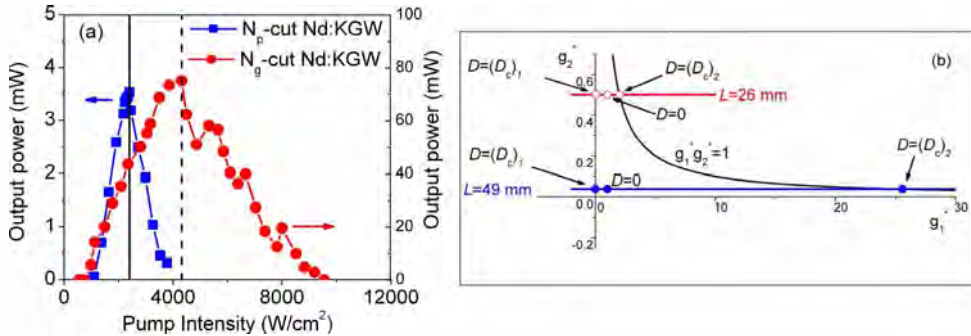


Fig. 3. (a) Measured output power as a function of the pump intensity ( $P_p/\pi w_p^2$ ) for  $N_p$ - (squares) and  $N_g$ - (circles) cut Nd:KGW lasers for a resonator length of  $L = 49$  mm and with  $L = 26$  mm respectively. Solid and dashed vertical lines indicate the critical pump intensity ( $P_p/\pi w_p^2$ )<sub>c</sub>, above which the output power drops, for  $N_p$ - and  $N_g$ -cut Nd:KGW, respectively. The laser resonators progress along the horizontal lines through the equivalent stability diagram (b) as the absolute value of the refractive power  $|D|$  of the thermal lens in the active element increases.  $(D_c)_1$  and  $(D_c)_2$  are then the characteristic refractive powers at which the resonators intersects the stability limits.

Here, the output power increases with increasing pump intensity up to a certain critical value,  $(P_p/\pi w_p^2)_c$ , above which the output power abruptly drops. This value of  $(P_p/\pi w_p^2)_c$  is equal to  $\approx 2.4$  kW/cm<sup>2</sup> and  $\approx 4.3$  kW/cm<sup>2</sup> for the  $N_p$ -cut and  $N_g$ -cut Nd:KGW lasers, respectively. According to [22], such a feature in the output power behaviour is observed when the laser resonator, due to the thermal lens induced in the active element, approaches the edge of stability region. Calculations in [22] show that, for the resonator configuration used in the experiment, there are two critical values of the thermal lens refractive power  $(D_c)_1 = 1/(L-l + ln^{-1})$  and  $(D_c)_2 = -1/(R-(L-l + ln^{-1}))$  (where  $L$  is the cavity length,  $l$  is the gain medium length, and  $n$  is the index of refraction of the gain medium) at which the laser resonator intersects the stability limits (Fig. 3(b)). For the  $N_p$ -cut Nd:KGW laser,  $(D_c)_1 = 20.8$  dptr and  $(D_c)_2 = -511.6$  dptr (the refractive index of Nd:KGW for the light polarization along the  $N_m$ -axis is  $n = 2.01$  [25]). Comparing  $(D_c)_1$  with  $(D_c)_2$  yields the relation  $|(D_c)_1| \ll |(D_c)_2|$ , and the abrupt drop in the output power for the  $N_p$ -cut Nd:KGW laser can be related to the focusing thermal lens as the critical value  $(D_c)_1$  will be reached at lower pump intensity compared with the critical value  $(D_c)_2$  of the defocusing thermal lens. Therefore, the sensitivity factor can be found to be  $(M_{N_p-cut})_{Nm} = (D_c)_1/(P_p/\pi w_p^2)_c = 0.87 \times 10^{-2}$  dptr/(W/cm<sup>2</sup>). For the  $N_g$ -cut Nd:KGW laser,  $(D_c)_1 = 39.9$  dptr and  $(D_c)_2 = -40.1$  dptr. Because the  $N_g$ -cut Nd:KGW crystals possesses a focusing thermal lens, the sensitivity factor can be found to be  $(M_{N_g-cut}) = (D_c)_1/(P_p/\pi w_p^2)_c = 0.92 \times 10^{-2}$  dptr/(W/cm<sup>2</sup>). However, it is not possible to assign this value of  $M$  to a certain ( $N_m$  or  $N_g$ ) direction.

It should be noted that the difference in the slope efficiencies of the two lasers does not influence the measurements of the thermal lens since the critical pump intensity depends only on the resonator parameters.

In Table 1 a summary of the results obtained for the thermal lensing sensitivity factors  $M$  and for the degree of astigmatism for the  $N_p$ -cut and  $N_g$ -cut Nd:KGW crystals are given. As can be seen from Table 1, the  $M$ -values for the  $N_p$ - and  $N_g$ -cut Nd:KGW obtained by the two

methods are in close agreement. Also it is clear that the  $N_p$ -cut Nd:KGW possesses a thermal lens having strong astigmatism with the degree of  $2.85 \text{ dptr}/(\text{W}/\text{cm}^2)$ . The ratio of the  $M$ -factors for  $N_m$ - and  $N_g$ -directions,  $(M_{N_p\text{-cut}})_{N_m}/(M_{N_p\text{-cut}})_{N_g}$  equals  $-0.425$ . The refractive powers of thermal lens for the  $N_g$ - and  $N_m$ -directions have different sign, minus and plus, respectively. In contrast, the thermal lens in the  $N_g$ -cut Nd:KGW displays weak astigmatism with the degree of  $0.35 \text{ dptr}/(\text{W}/\text{cm}^2)$ , and the value of  $(M_{N_g\text{-cut}})_{N_m}/(M_{N_g\text{-cut}})_{N_p}$  here is found to be  $1.4$ . This implies that the  $N_g$ -cut Nd:KGW laser, as compared to the  $N_p$ -cut Nd:KGW one, can operate at significantly higher pump intensities.

**Table 1. Comparison of the thermal lensing sensitivity factors  $M$  and thermal lens' degree of astigmatism for the  $N_p$ -cut and  $N_g$ -cut Nd:KGW crystals. The factor  $M$  is deduced with two different methods, namely: (i) analysis of the laser output beam size in dependence on the distance from the output coupler at different pump intensity; and (ii) analysis of the laser output power as a function of the pump intensity.**

Direction	$M$ , dptr/(W/cm <sup>2</sup> )			
	$N_p$ -cut Nd:KGW		$N_g$ -cut Nd:KGW	
	(i)	(ii)	(i)	(ii)
along $N_m$	$0.85 \times 10^{-2}$	$0.87 \times 10^{-2}$	$1.2 \times 10^{-2}$	$0.92 \times 10^{-2}$
along $N_p$	–	–	$0.85 \times 10^{-2}$	–
along $N_g$	$-2.0 \times 10^{-2}$	–	–	–
Degree of astigmatism, dptr/(W/cm <sup>2</sup> )	2.85		0.35	

In support of this statement it was observed in our experiments that the 7at.%-doped  $N_p$ -cut Nd:KGW laser could not operate in the  $cw$  regime, and laser oscillation was only obtained under quasi- $cw$  pumping. In contrast, the 7at.%-doped  $N_g$ -cut Nd:KGW laser easily demonstrated  $cw$  oscillation with the same cavity configuration. It should be noted that the characteristics of the thermal lens in the  $N_g$ - and  $N_p$ -cut diode-pumped Nd:KGW crystals obtained here are in good agreement with the results of thermal lens studies in  $N_g$ - and  $N_p$ -cut Nd:KGW crystals under flashlamp-pumping at a wavelength of  $1.067 \mu\text{m}$  [16]. Moreover, results of our measurements of the thermal lens in  $N_g$ -cut Nd:KGW are also consistent with the observations of the thermal lens in Yb:KGW crystal cut along the same direction [17]. Positive values of the thermal lens in vertical and horizontal directions (unfortunately, these directions were not assigned with the direction of polarization of the laser emission) were reported for this crystal [17]. Results in [11] on the thermal lens measurements in the  $N_p$ -cut Nd:KGW demonstrated strong negative thermal lens in the plane of polarization and the positive one in the perpendicular plane. These observations (regarding the sign of the thermal lens) are in contrast to the one made in [16] and in the present paper. Currently we cannot explain such discrepancy in the signs of the thermal lens.

Several factors contribute thermal lensing effect in the solid-state lasers: temperature- and stress-dependent variations of refractive index, bowling of the crystal faces under thermal expansion [18], specific diode beam profiles and collimation optics [17]. Thermo-optic coefficient  $dn/dT$  is the more significant among them especially in diode-pumped lasers [18]. Therefore, one can compare thermal lens sign with the one of  $dn/dT$  coefficient for the laser polarization (in our experiment it is parallel to the  $N_m$ -axis for both crystals). Our results on thermal lens signs are in correlation with [13], where dependence of  $dn/dT$  coefficient on the beam propagation direction was observed, with the negative value for light propagation along the  $N_p$ -axis and positive value for light propagation along the  $N_g$ -axis for light polarization along  $N_m$ -axis at  $1.06 \mu\text{m}$ ; and [14], where  $dn/dT$  coefficient (at  $435.8$  and  $632.8 \text{ nm}$ ) for light polarization along  $N_g$ -axis was found to be negative while the two other values for light polarizations along  $N_p$  and  $N_m$  axes were positive [14].

We suppose that the laser performance of Nd:KGW crystal under diode pumping can be improved by cutting the crystal along some directions in the  $N_p$ - $N_g$  plane for which thermal lens would be positive or close to zero with a weak astigmatism resulting in near-symmetric output beam.

#### 4 Conclusion

A comparative study of the thermal lensing in diode laser pumped  $N_g$ - and  $N_p$ -cut Nd:KGW laser crystals was performed for laser emission polarized along the principle refractive axis  $N_m$ . The thermal lens in  $N_g$ -cut Nd:KG was found to have a weak astigmatism with positive refractive power for both the  $N_m$ - and  $N_p$ -directions. In contrast, the thermal lens in  $N_p$ -cut Nd:KGW possesses strong astigmatism with refractive powers of different signs for the  $N_g$ - and  $N_m$ -directions. The degree of astigmatism was found to be considerably weaker for the  $N_g$ -cut Nd:KGW in comparison with the  $N_p$ -cut one: 0.35 dptr/(W/cm<sup>2</sup>) and 2.85 dptr/(W/cm<sup>2</sup>), respectively. The factor  $M$ , the thermal lens sensitivity, for both configurations has also been studied and characterised. The ratios of the  $M$ -factors in the plane of polarisation and in the perpendicular plane were evaluated to be  $(M_{N_g-cut})_{Nm}/(M_{N_g-cut})_{Np} = 1.4$  and  $(M_{Np-cut})_{Nm}/(M_{Np-cut})_{Ng} = -0.425$  for the  $N_g$ - and  $N_p$ -cut Nd:KGW, respectively. Thus the 'athermal'  $N_g$ -cut crystal configuration shows significant promise specifically for diode-pumped 1.3  $\mu\text{m}$  Nd:KGW lasers operating at high pump intensities.